Activation of the Nickel-Deficient Carbon Monoxide Dehydrogenase from *Rhodospirillum rubrum*: Kinetic Characterization and Reductant Requirement†

Scott A. Ensign, Michael J. Campbell, and Paul W. Ludden*

Department of Biochemistry, College of Agricultural and Life Sciences, University of Wisconsin—Madison, Madison, Wisconsin 53706

Received August 21, 1989; Revised Manuscript Received October 25, 1989

ABSTRACT: The requirements for and kinetics of the activation of the nickel-deficient (apo) CO dehydrogenase from *Rhodospirillum rubrum* by exogenous nickel have been investigated. The activation is strictly dependent upon the presence of a low-potential one-electron reductant. Sodium dithionite and reduced methylviologen ($E^{\circ\prime} = -440$ mV) are suitable reductants, whereas reduced indigo carmine ($E^{\circ\prime} = -125$ mV) and the two-electron reductants sodium borohydride, NADH, and dithiothreitol are ineffective in stimulating activation. The midpoint potential for activation was observed at approximately −475 mV. The ability of a reductant to stimulate activation is correlated with the reduced state of the enzyme Fe_4–S_4 centers. The activation follows apparent first-order kinetics in a saturable fashion, yielding a rate constant of 0.157 min^{-1} at saturating concentration of nickel. The initial rate at which the enzyme is activated by $NiCl_2$ is also a saturable process, yielding a dissociation constant (K_D) of 755 μM for the initial association of nickel and enzyme. Cadmium(II), zinc(II), cobalt(II), and iron(II) are competitive inhibitors of nickel activation with inhibition constants of 2.44, 4.16, 175, and 349 μM, respectively. Manganese(II), calcium(II), and magnesium(II) exhibit no inhibition of activation.

Two classes of nickel-containing CO dehydrogenases have been isolated and characterized from anaerobic bacteria. The CO dehydrogenases purified from acetogenic and methanogenic bacteria are large, multimeric, O_2-labile, nickel- and iron–sulfur-containing enzymes whose principle function is the synthesis and/or degradation of acetyl coenzyme A (acetyl-CoA)[1] (Wood et al., 1986; Terlesky et al., 1986; Krzycki & Zeikus, 1984). The CO dehydrogenase from the photosynthetic bacterium *Rhodospirillum rubrum* is, in contrast, an O_2-labile, monomeric, nickel- and iron–sulfur-containing enzyme of 62 000 molecular weight which apparently functions solely to oxidize CO to CO_2 (Bonam & Ludden, 1987). In *R. rubrum*, CO dehydrogenase and a CO-insensitive hydrogenase are specifically induced by CO, suggesting that the physiological function of CO dehydrogenase is the oxidation of CO coupled to the reduction of protons by hydrogenase (Bonam et al., 1989).

Exposure of *R. rubrum* to CO during growth on medium depleted of nickel results in the synthesis of a nickel-free form of CO dehydrogenase which can be activated both in vivo and in vitro by the addition of $NiCl_2$ (Bonam et al., 1988). The purified nickel-free enzyme ("apo-CO dehydrogenase"), which is identical with the holoenzyme in molecular weight and iron content, is catalytically inactive and activated to a specific activity comparable to the holoenzyme upon the addition of $NiCl_2$ (Bonam et al., 1988; Ensign et al., 1989a). The CO analogue cyanide binds to and inhibits holo-CO dehydrogenase but not apo-CO dehydrogenase (Ensign et al., 1989b), and the Fe–S centers of the oxidized holoenzyme but not the oxidized apoenzyme are reduced by CO (Ensign et al., 1989a), implicating nickel as the site of CO binding and as the mediator in electron flow to the enzyme Fe–S centers.

Although nickel is recognized as a cofactor in at least four classes of enzymes [for reviews, see Hausinger (1987) and Walsh and Orme-Johnson (1987)], little is known about the mechanisms of nickel insertion to form active holoenzymes, or the detailed structures of the nickel centers. With the exception of *R. rubrum* CO dehydrogenase, nickel-free forms of other nickel enzymes which can be activated in vitro by the addition of nickel have not been reported. Nickel has been successfully substituted for the native iron atom of rubredoxins from three species of *Desulfovibrio*, and the nickel-substituted proteins have been shown to mimic bacterial nickel hydrogenase reactivity with respect to hydrogen production, deuterium–proton exchange, and inhibition by CO (Saint-Martin et al., 1988). There is evidence that some bacteria and algae accumulate a nickel-deficient form of urease when grown on nickel-deficient medium, but the inactive proteins have not been purified, and attempts to reconstitute urease activity in vitro by the addition of nickel have proven unsuccessful (Mobley & Hausinger, 1989). Clearly, the existence of a nickel-free form of CO dehydrogenase from *R. rubrum* provides a valuable tool in the elucidation of the structure and function of the nickel site of this novel metalloenzyme. An understanding of the requirements for and kinetics of the insertion of nickel into the vacant site of the apoenzyme is of integral importance in this elucidation. In this paper, we present a detailed kinetic study of the activation of nickel-deficient apo-CO dehydrogenase by nickel(II), characterize the transition metals cobalt(II), iron(II), zinc(II), and cadmium(II) as competitive inhibitors of activation, and demonstrate that activation is dependent upon the presence of a low-potential one-electron reductant.

† This research was supported by the College of Agricultural and Life Sciences at the University of Wisconsin—Madison and by Grant DE-FG02-87ER13691 from the U.S. Department of Energy. S.A.E. was supported by Training Grant 5T32GM07215-14 from the National Institutes of Health. DOE support does not constitute an endorsement by DOE of the views expressed in this paper.

* Address correspondence to this author.

[1] Abbreviations: acetyl-CoA, acetyl coenzyme A; CODH, carbon monoxide dehydrogenase; EPR, electron paramagnetic resonance; DTT, dithiothreitol.

0006-2960/90/0429-2162$02.50/0

Materials and Methods

Materials

CO (99.99+%) and N_2 (99.998+%) were purchased from Matheson (Chicago, IL). Gases were stripped of trace O_2 by passage over a heated copper-based catalyst (R3-11, Chemical Dynamics Corp., South Plainsfield, NJ). Ultrapure $NiCl_2$, $CoCl_2$, $Fe(NO_3)_3$, $Cd(NO_3)_2$, $ZnCl_2$, $CuCl_2$, $CaCl_2$, and $MgSO_4$ were obtained from Aldrich Chemical Co. (Milwaukee, WI). Methylviologen, indigo carmine, sodium borohydride, and NADH were obtained from Sigma Chemical Co. (St. Louis, MO).

Methods

Cell Growth and Protein Purification. R. rubrum (ATCC 11170) cells for apo- and holo-CO dehydrogenase purification were grown as described previously (Ensign et al., 1989b). Holo- and apo-CO dehydrogenases were purified as described (Bonam & Ludden, 1987; Bonam et al., 1988; Ensign et al., 1989b). The final step of purification, preparative-scale native gel electrophoresis, yields two bands of CODH activity referred to as peaks 1 and 2 (Bonam & Ludden, 1987). The peak 1 fractions of both holo- and apo-CO dehydrogenase are the forms used for the experiments described in this and previous papers. Holo-CO dehydrogenase contained 7.4 mol of iron and 1.1 mol of nickel/mol of enzyme as determined by plasma emission spectrophotometry (Ensign et al., 1989a) and had a specific activity of 4440 units/mg (1 unit = 1 μmol of CO oxidized/min). Purified apo-CO dehydrogenase contained 7.4 mol of iron and <0.02 mol of nickel/mol of protein and had a specific activity of 46 units/mg. Protein concentration was determined by the method of Peterson (1977) using Sigma grade A bovine serum albumin as standard.

Nickel Activation of Apo-CO Dehydrogenase for Kinetic Studies. Activations of apo-CO dehydrogenase were performed in stoppered 25-mL polyethylene serum vials (Wheaton) containing 2-mL total volume activation assay mixture. Prior to usage, the vials were stored for several days in an anaerobic glovebox containing less than 1 ppm of oxygen (Vacuum/Atmospheres Dri-Lab glovebox, Model HE-493) and then rinsed with buffer containing 0.1 mM dithionite to remove trace oxygen bound to the plastic. The assay mixture contained 0.1 mM methylviologen in 100 mM MOPS buffer, pH 7.5. An appropriate volume of 10 mM dithionite was added to fully reduce the methylviologen in the assay vial, leaving a 0.01 mM excess of reduced dithionite. Apo-CO dehydrogenase (0.71 nmol) was added to the vial, and after 5-min preincubation at 25 °C, an appropriate volume of degassed $NiCl_2$ stock solution (0.01, 0.1, or 1 M) was added to initiate the activation. Samples (2–8 μL) were removed at the desired time points (including at t_0 prior to addition of $NiCl_2$), and CO oxidizing activity was measured spectrophotometrically at 25 °C and pH 7.5 using the CO-dependent methylviologen reduction assay previously described (Ensign et al., 1989b). Cobalt inhibition studies were performed in an analogous fashion, with aliquots of stock solutions of premixed $CoCl_2$ and $NiCl_2$ added to initiate the activations. For iron inhibition studies, a stock solution of Fe(III) [obtained as $Fe(NO_3)_3$] was reduced to Fe(II) with dithionite. Aliquots of Fe(II) and $NiCl_2$ solutions were simultaneously injected to initiate activations. Activations in the presence of zinc (or cadmium) were initiated by the simultaneous injections of $NiCl_2$ and $ZnCl_2$ [or $Cd(NO_3)_2$] solutions. Hamilton syringes were used for all enzyme, dithionite, and metal ion additions.

CO Dehydrogenase Oxidation. Oxidation of dithionite-reduced CO dehydrogenase was carried out in the anaerobic box. Proteins were stripped of dithionite by passage over a 1 × 10 cm column of Sephadex G-25 and then oxidized by the addition of 3 mM (final concentration) indigo carmine. Indigo carmine was removed by passage over a 5 × 15 cm column containing a 10-cm layer of AG 1-X8 ion-exchange resin (Bio-Rad) located above a 5-cm layer of Sephadex G-25. The buffer was 100 mM MOPS, pH 7.5, in all steps.

Preparation of Other Proteins. Hydrogenase I purified from *Clostridium pasteurianum* (>90% pure) was a gift from Duane Bonam, University of Georgia, Athens, GA. Hydrogenase was stripped of dithionite on a 1 × 10 cm column of Sephadex G-25 in the anaerobic box prior to use. The enzyme thus prepared had a specific activity of 3200 μmol of H_2 oxidized min^{-1} (mg of protein)$^{-1}$ when assayed at pH 8.0 using methylene blue as electron acceptor. Flavodoxin purified from *Azotobacter vinelandii* (>95% pure) was a gift from Vinod Shah in our laboratory, and ferredoxins I and II purified from *R. rubrum* (~75% pure) were gifts from Scott Murrell in our laboratory. Flavodoxin and ferredoxins were aerobically exchanged into 100 mM MOPS buffer, pH 7.5, on 1 × 10 cm columns of Sephadex G-25 and then degassed and allowed to equilibrate in the anaerobic box prior to use.

Kinetic Analysis. Apparent first-order rate constants for the activation of apo-CO dehydrogenase at a given $[NiCl_2]$ were derived by fitting plots of activity vs time to the equation

$$\ln (\text{act.}_{\max} - \text{act.}_t) = \ln (\text{act.}_{\max} - \text{act.}_{\text{res}}) - k_{\text{obs}}t \quad (1)$$

Equation 1 was obtained by rearrangement of the first-order rate law:

$$\text{act.}_t = (\text{act.}_{\max} - \text{act.}_{\text{res}})(1 - e^{-k_{\text{obs}}t}) + \text{act.}_{\text{res}} \quad (2)$$

act._t is the activity at time t after the initiation of activation, act._{res} is the residual activity of the unactivated apoenzyme, and $\text{act.}_{\max}$ is the activity of the fully activated enzyme. Initial rates of activation (reported as the increase in specific activity per minute) were taken from the slope of plots of activity vs time for the first 3.5 min of activation. The dissociation constant (K_D) for nickel and the inhibition constants (K_I) for other metal ions were derived by fitting the initial rates to the following equations for rectangular hyperbolas using the computer programs described by Cleland (1979):

absence of inhibitor

$$v = \frac{V[Ni^{2+}]}{K_D + [Ni^{2+}]} \quad (3)$$

presence of inhibitor

$$v = \frac{V[Ni^{2+}]}{K_D(1 + [I]/K_I) + [Ni^{2+}]} \quad (4)$$

v is the rate of initial activation, V is the rate of initial activation at saturating nickel, and $[Ni^{2+}]$ and [I] are the concentrations of nickel and the inhibitory metal ion, respectively.

Numerical Constants. Solution potentials of assay mixtures containing partially reduced redox dyes were estimated from the Nernst equation, using the approximation of 0.059 for $2.303RT/F$ at 25 °C (Dutton, 1978). The midpoint potential of methylviologen was taken as −440 mV at pH 7.5 (Clark, 1960; Prince et al., 1981).

Results

Reductant Requirement for Activation of Apo-CO Dehydrogenase. Previous studies on the activation of apo-CO

Table I: Effects of Various Reducing Agents on the Activation of Apo-CODH by $NiCl_2$[a]

reductant	activity, t = 5 min	activity, t = 15 min	x-fold activation at 15 min
none	41.92	43.5	1.01
0.3 mM dithionite	1805	2482	57.7
0.1 mM MV[b]	1013	2554	59.4
0.1 mM IC[c]	41.92	43.5	1.01
2 mM NADH	35.5	37.0	0.86
1 mM $NaBH_4$	45.5	44.4	1.03
0.5 mM DTT	27.4	29.0	0.67
H_2	41.92	38.65	0.90
CO	38.7	40.3	0.94

[a] Apo-CODH was oxidized as described under Materials and Methods. Incubation vials containing 20 μg of enzyme and specified reductant in 1-mL total volume MOPS buffer, pH 7.5, were set up in the glovebox. After a 2-min preincubation, activations were initiated by the addition of 5 mM $NiCl_2$. Samples were withdrawn at 5 and 15 min after initiation of activation, and CO oxidizing activity was measured spectrophotometrically. Activity is reported as micromoles of CO oxidized per minute per milligram. The activity of the untreated apoenzyme was 43.0 units/mg. [b] Methylviologen was determined spectrophotometrically to be 93.6% reduced after titration with 10 mM dithionite, with an estimated potential of −509 mV. [c] Indigo carmine was determined spectrophotometrically to be 97.6% reduced after titration with 10 mM dithionite, with an estimated potential of −220 mV.

dehydrogenase were performed in the presence of the low-potential reductant dithionite in order to maintain anaerobic conditions (Bonam et al., 1988; Ensign et al., 1989a). Under these conditions, the Fe–S centers of both apo- and holo-CO dehydrogenase are in the reduced state as determined by UV/visible (Bonam & Ludden, 1987; Ensign et al., 1989a) and EPR (Bonam & Ludden, 1987; Bonam et al., 1988) spectroscopy. To establish whether the oxidized form of apo-CO dehydrogenase is a substrate for nickel activation, 5 mM $NiCl_2$ was added to indigo carmine oxidized apoenzyme and activity followed over a 15-min time course. As shown in Table I, no activation of the oxidized enzyme occurred unless a suitable reductant was added to the activation mixture. Both dithionite and reduced methylviologen ($E^{\circ\prime}$ = −440 mV) were effective reductants whereas reduced indigo carmine ($E^{\circ\prime}$ = −125 mV) was an ineffective reductant. NADH and $NaBH_4$, low-potential two-electron reductants, were ineffective reductants as was DTT, which is routinely used to reduce disulfide bridges in proteins (Cleland, 1964). Hydrogen gas was also an ineffective reductant, as was CO, the substrate for the holoenzyme.

The data presented in Table I indicate that the Fe–S centers of apo-CO dehydrogenase must be in the reduced state for activation to occur. $NaBH_4$, NADH, and H_2 were unable to reduce the apoenzyme Fe–S centers as determined by UV/visible spectrometry. Incubation of either holo- or apo-CO dehydrogenase in the presence of $NaBH_4$ or NADH led to no loss of enzyme activity, demonstrating that they have no deleterious effects on enzyme activity.

In order to more quantitatively estimate the midpoint potential required for activation of the apoenzyme, the solution potential was set by adding aliquots of 10 mM dithionite to activation mixtures containing 0.1 mM methylviologen and oxidized apoenzyme. A variety of activation mixtures were obtained with estimated potentials between −375 and −525 mV. As shown in Figure 1, at potentials above −400 mV very little activation of the apoenzyme (as measured by the rate of activation during the first 5 min after the addition of 5 mM $NiCl_2$) occurred. As the potential was progressively lowered, greater rates of activation were attained, with maximal rates

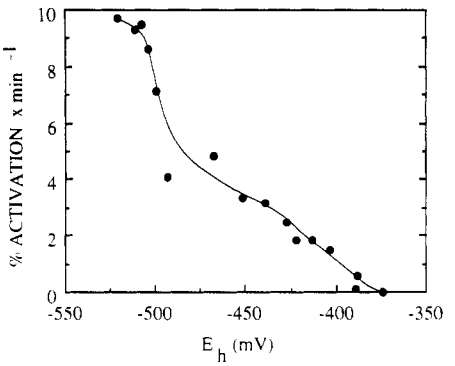

FIGURE 1: Effect of solution potential on the rate of apo-CO dehydrogenase activation. Activations were performed in 1.5-mL anaerobic cuvettes containing 1-mL total volume of 0.1 mM methylviologen in 100 mM MOPS buffer, pH 7.5. The absorbance values of fully oxidized and fully dithionite-reduced methylviologen were determined spectrophotometrically at 578 nm. Aliquots of 10 mM dithionite were added to oxidized apo-CODH (0.36 nmol) in activation cuvettes to obtain several semireduced states. Five millimolar $NiCl_2$ was added to initiate activations, and the absorbance of the semireduced cuvettes at 578 nm and the activity of the activated enzymes were measured at t = 5 min. The ratio of oxidized to reduced methylviologen in the activation cuvettes was determined by comparing the absorbance values at 578 nm to the values of fully oxidized and reduced methylviologen, and the solution potential was calculated from the Nernst equation. The rate of activation is expressed as the percentage of apoenzyme activated per minute. The line through the data points was drawn as a best fit by eye.

occurring at potentials below −500 mV. A midpoint potential of ∼−475 mV for the rate of activation of apo-CO dehydrogenase was estimated from the plot in Figure 1.

In describing the effect of solution potential on the activation of the apoenzyme, a distinction should be made between the *rate* of activation and final *extent* of activation. Although the rate of activation was quite slow at potentials between −425 and −375 mV, the apoenzyme mixtures incubated with nickel at these potentials were fully activated if the activations were allowed to proceed to equilibrium (>2 h). Our previous work has shown that electrons are reversibly transferred between the oxidized and reduced forms of holo- and apo-CO dehydrogenase through the mediating action of methylviologen (Ensign et al., 1989a). Given the probable similarities in the midpoint potentials of methylviologen and the Fe–S centers of apo- and holo-CO dehydrogenase, and that the apoenzyme must be in the reduced state in order to bind nickel and be converted to the holoenzyme, it is apparent that even at low ratios of reduced to oxidized methylviologen the majority of the apoenzyme will be converted to holoenzyme given sufficient time. With methylviologen as reductant, the dependence of solution potential on activation is manifest as a kinetic and not an equilibrium effect.

Although H_2 was by itself an ineffective reductant for the reduction and activation of apo-CO dehydrogenase, H_2 oxidation could be coupled to activation in the presence of suitable mediating proteins. The purified bidirectional hydrogenase I from *Clostridium pasteurianum* was used to catalyze the oxidation of H_2. As shown in Figure 2, incubation of oxidized apo-CO dehydrogenase with hydrogenase and H_2 resulted in no activation of the apoenzyme, indicating that direct electron transfer between the two proteins does not occur. However, when the oxidized forms of purified ferredoxins I and II from *R. rubrum* or purified flavodoxin from *Azotobacter vinelandii* were added, activation of the apoenzyme occurred (Figure 2). The lag in the time required to attain maximal rates of activation with these electron carrier proteins is attributed to the time required for the intermediate proteins to become suffi-

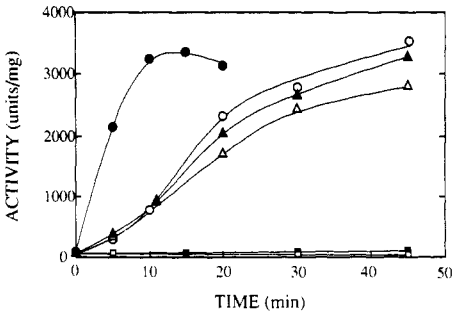

FIGURE 2: H_2- and hydrogenase-dependent activation of apo-CO dehydrogenase mediated by *R. rubrum* ferredoxins and *A. vinelandii* flavodoxin. Activation vials (9 mL) contained 1-mL total volume of 100 mM MOPS buffer, pH 7.5, and 0.26 nmol of indigo carmine oxidized apo-CO dehydrogenase under either 101 kPa of N_2 or H_2. Activations were initiated by the addition of $NiCl_2$ to 5 mM concentration: (●) 0.1 mM dithionite added as reductant; (■) no reductant added; (□) 101 kPa of H_2 and 0.026 nmol of *C. pasteurianum* H_2ase I added; (○) 101 kPa of H_2, 0.026 nmol of *C. pasteurianum* H_2ase I, and 50 nmol of *A. vinelandii* flavodoxin added; (▲) 101 kPa of H_2, 0.026 nmol of *C. pasteurianum* H_2ase I, and 50 nmol of *R. rubrum* ferredoxin II added; (△) 101 kPa of H_2, 0.026 nmol of *C. pasteurianum* H_2ase I, and 50 nmol of *R. rubrum* ferredoxin I added. Samples (2–10 μL) were removed at the indicated times, and CO oxidizing activity was measured spectrophotometrically.

ciently reduced by hydrogenase to drive the transfer of electrons to CO dehydrogenase.

Oxidized apo-CO dehydrogenase is not a substrate for nickel activation; however, it is possible that nickel binds stably at the nickel site of the oxidized enzyme but not in the correct configuration for formation of an active holoenzyme and that activation occurs upon addition of reductant. To resolve this question, oxidized apoenzyme was incubated with 5 mM $NiCl_2$ for 30 min, and unbound nickel was then removed by gel filtration on a 25 × 1 cm column of Sephadex G-25. Subsequent assay of the enzyme showed no increase in activity over the untreated apoenzyme, even after reduction with dithionite. Addition of 5 mM $NiCl_2$ to the now-reduced enzyme resulted in full activation within 20 min. These results indicate that nickel does not bind specifically to the oxidized apoenzyme.

Kinetics of Activation of Apo-CO Dehydrogenase. For kinetic analysis of nickel activation, dithionite-reduced methylviologen was chosen as the reductant. Both dithionite and reduced methylviologen give comparable rates of activation at a given concentration of $NiCl_2$; however, upon prolonged incubation, solutions of $NiCl_2$ incubated with dithionite form a gray precipitate believed to be Ni(0). This precipitate was observed only during the time frame of the kinetic experiments at dithionite concentrations greater than 0.05 mM. To avoid depletion of Ni(II) in solution according to this reaction, a fully reduced solution of methylviologen containing a slight excess of dithionite (0.01 mM) was used. Following this protocol, no precipitate formed, and solutions stayed fully reduced throughout the time frame of the experiments.

The time and $[NiCl_2]$ dependence on the rate of activation of apo-CO dehydrogenase is shown in Figure 3. Maximal rates of activation were obtained with $NiCl_2$ concentrations of 2.5–5 mM, and at these concentrations, the activations were essentially complete within 15 min of addition of $NiCl_2$. At all concentrations of $NiCl_2$ studied, the activations reached the same specific activity (within ~5%) if allowed to proceed to completion (>3 h required at 25 μM $NiCl_2$; data not shown). Complete activation at the low $NiCl_2$ concentrations was dependent upon performing the activations in polyethylene vials. When the activations were performed in glass serum vials, the activations reached stable, lower than maximal

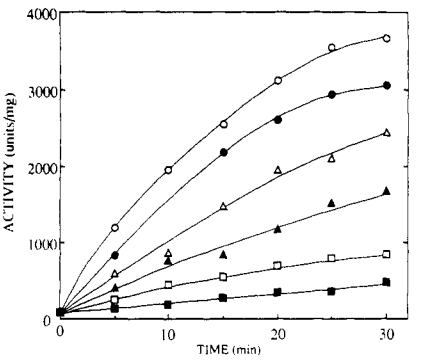

FIGURE 3: Dependence of apo-CO dehydrogenase activation on nickel(II) concentration. Activations were initiated as described under Materials and Methods. At 5-min intervals, samples of enzyme (2–8 μL) were removed, and CO oxidizing activity was measured spectrophotometrically. The plot shows activity vs time for the first 30 min of activation; $NiCl_2$ concentrations were (○) 1.0, (●) 0.50, (△) 0.25, (▲) 0.10, (□) 0.050, and (■) 0.025 mM.

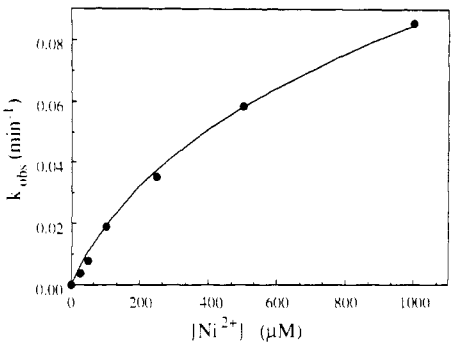

FIGURE 4: Relationship between apparent first-order rate constants and nickel(II) concentration. Apparent first-order rate constants (k_{obs}) at various concentrations of $NiCl_2$ were derived from the data presented in Figure 3 as described under Materials and Methods.

(~20–40% of maximal activity) activity levels after approximately 30 min of incubation. This is most likely due to the depletion of $NiCl_2$ by adsorption to the glass surface. The use of glass vials had little effect on the rate of activation at $NiCl_2$ concentrations above 1 mM. Lowering the MOPS buffer concentration from 100 to 10 mM had no effect on the rate of activation at 0.050 mM $NiCl_2$, indicating that binding of nickel to the buffer is not a problem over the time course of these assays.

A quantitative analysis of the data presented in Figure 3 demonstrates that the activation of apo-CO dehydrogenase is a pseudo-first-order process. When the data in Figure 3 are replotted in semi-logarithmic form (using eq 1 presented under Materials and Methods), the plots are linear and intersect at a common point on the y axis (correlation coefficients of 0.977, 0.981, 0.983, 0.987, 0.994, and 0.984 for $NiCl_2$ concentrations of 25, 50, 100, 250, 500, and 1000 μM, respectively). Apparent first-order rate constants were obtained from the slopes of these plots. A plot of the rate constants vs $[NiCl_2]$ (Figure 4) is hyperbolic, demonstrating that the activation is a saturable process with respect to nickel. Fitting the data to a hyperbola ($r = 0.999$) gives the maximal rate constant (k_{max}) for activation of 0.157 ± 0.009 min^{-1} at saturating nickel. This fit also provides an estimate of the dissociation constant (K_D) for nickel of 835 ± 83 μM.

Although the activation of apo-CO dehydrogenase is a pseudo-first-order process, activations were found to remain linear for at least 3.5 min at $NiCl_2$ concentrations up to 5 mM (data not shown). This observation was used as a basis for kinetically characterizing the rate of activation during its linear

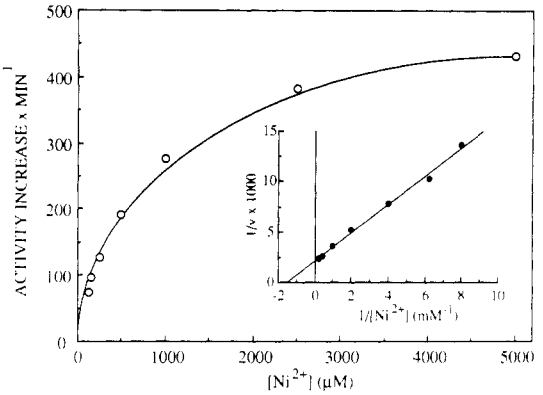

FIGURE 5: Rate of apo-CO dehydrogenase activation at various concentrations of nickel(II). The rate of specific activity increase is plotted vs [Ni^{2+}]. The inset shows the data replotted in double-reciprocal form.

portion (taken from the slopes of the plots of activity vs time for the first 3.5 min of activation) as a function of $NiCl_2$ concentration. As shown in Figure 5, the rate of initial activation is a saturable process. The data in Figure 5 replotted in double-reciprocal fashion yield a linear plot (inset to Figure 5), demonstrating that the activation conforms to the equations describing Michaelis–Menten kinetics. A dissociation constant for nickel of 755 ± 38 μM was calculated from a fit of the data. This value agrees well with the binding constant of 835 μM obtained from the plot of first-order rate constants vs [$NiCl_2$] (Figure 4), demonstrating that both the first-order and initial rate analyses are valid methods for kinetically characterizing the activation of the apoenzyme.

Effects of Divalent Metal Ions on Nickel Activation. The kinetic analysis described above was applied to characterize possible inhibition of nickel activation by closely related transition metals. Cobalt, zinc, and iron have previously been shown to remain stably associated in stoichiometric ratios (~1:1 mole ratio) with dithionite-reduced apo-CO dehydrogenase but with no increase in specific activity (Ensign et al., 1989a). Subsequent treatment of these enzymes with $NiCl_2$ resulted in no activity increase, indicating that the substitute metals have stably bound at and blocked the nickel site (Ensign et al., 1989a). The effect of these and other metals on the rate of nickel activation was investigated by following activity increase vs time during the linear region of activation after the simultaneous addition of nickel and the possible inhibitory analogue. A double-reciprocal plot of activity increase vs [$NiCl_2$] in the presence of various concentrations of $CoCl_2$ reveals that cobalt is a competitive inhibitor of activation (Figure 6). An inhibition constant for $CoCl_2$ of 175 ± 18 μM was calculated from a fit of the experimental data. Similar kinetic analyses with Fe(II), Zn(II), and Cd(II) reveal that they are also competitive inhibitors of activation with inhibition constants varying from 349 to 2.44 μM (Table II). Calcium(II), Mg(II), and Mn(II) exhibited no inhibition even when present in concentrations 100-fold in excess of nickel. Copper(II) was found to inhibit activation; however, incubation of either the holo- or the apoenzyme with low concentrations (<2 μM) of $CuCl_2$ led to rapid loss of CO oxidizing activity. Copper(II) was, therefore, not further characterized as an inhibitor of activation.

To determine whether the inhibitory metal ions cobalt and zinc bind stably to the oxidized apoenzyme, apo-CO dehydrogenase was oxidized and incubated with a solution of either $ZnCl_2$ (0.25 or 0.50 mM) or $CoCl_2$ (5.0 mM) for 30 min, after which unbound metal ions were separated by Sephadex G-25 gel filtration chromatography. After reduction

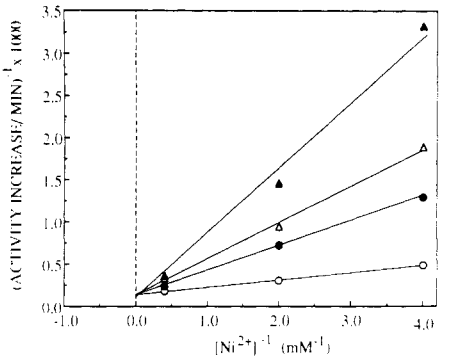

FIGURE 6: Competitive inhibition of apo-CO dehydrogenase activation by cobalt(II). Activations were performed as described under Materials and Methods. Samples (2–8 μL) were removed, and activity was measured spectrophotometrically at t = 0, 1.5, and 3.5 min after addition of $CoCl_2$ and $NiCl_2$. The concentrations of $CoCl_2$ present were (▲) 1.0, (△) 0.70, (●) 0.40, and (○) 0 mM. The lines through the data points were drawn manually; the value of K_I was determined by computer fit of the data as described under Materials and Methods.

Table II: Divalent Metal Ion Inhibition of Apo-CO Dehydrogenase Activation[a]

inhibitor	K_I (μM)
$CoCl_2$[b]	175 ± 18
$Fe(NO_3)_2$[c]	349 ± 123
$ZnCl_2$[d]	4.16 ± 0.72
$Cd(NO_3)_2$[e]	2.44 ± 0.90
$MgSO_4$, $CaCl_2$, or $MnCl_2$	ND[f]

[a] Activations were performed as described under Materials and Methods. Samples (2–8 μL) were removed, and activity was measured spectrophotometrically at t = 0 and 1.5 and 3.5 min after initiation of activation by addition of $NiCl_2$ and the inhibitory metal ion. Activations in the presence of Zn(II) and Cd(II) were assayed at t = 0, 0.75, and 1.5 min. [b] $NiCl_2$ concentrations of 250, 500, and 2500 μM and $CoCl_2$ concentrations of 0, 400, 700, and 1000 μM were used in determining K_I. [c] $NiCl_2$ concentrations of 250, 500, and 2500 μM and $Fe(NO_3)_2$ concentrations of 0, 400, 700, and 1000 μM were used in determining K_I. [d] $NiCl_2$ concentrations of 250, 500, 1000, and 2500 μM and $ZnCl_2$ concentrations of 0, 12, 15, and 18 μM were used in determining K_I. [e] $NiCl_2$ concentrations of 250, 500, 1000, and 2500 μM and $CdCl_2$ concentrations of 0 and 6.0 μM were used in determining the K_I. [f] No detectable inhibition at 5000 μM M^{2+} and 50 μM $NiCl_2$.

by dithionite, the $CoCl_2$-treated apoenzyme was activated to the same final specific activity as the nickel-activated apoenzyme upon the addition of 5 mM $NiCl_2$. The activation of the apoenzyme treated with 0.25 mM $ZnCl_2$ was inhibited 50% after desalting, and the activation of the apoenzyme treated with 0.50 mM $ZnCl_2$ was inhibited 75%. By way of comparison, the activation of protein samples which had been incubated with 5 mM $CoCl_2$ or 0.25 mM $ZnCl_2$ in the presence of 0.2 mM dithionite was fully inhibited after separation of unbound metals. These results indicate that cobalt(II), like nickel(II), has little or no affinity for the nickel site of the oxidized enzyme, while zinc(II) appears to have some binding affinity.

Discussion

The work described in this paper demonstrates that a low-potential one-electron reductant is strictly required for the insertion of nickel into the nickel-deficient CO dehydrogenase from *R. rubrum*. This observation, along with the estimated potential of ~−475 mV for activation and the ability of low-potential electron carrier proteins (ferredoxin and flavodoxin) to serve as reductants, suggests that the Fe–S centers of the apoenzyme must be reduced for activation to occur. Alternate explanations are that a disulfide linkage present in the oxidized apoenzyme must be reduced to free sulfhydryls, possibly as

Scheme I

$$E + Ni \underset{k_2}{\overset{k_1}{\rightleftharpoons}} E{\cdot}Ni \xrightarrow{k_{max}} E{\cdot}Ni^*$$

step 1 step 2

ligands for nickel, or that nickel(II) must necessarily be reduced to Ni(0) or Ni(I) prior to incorporation into the apoenzyme. The involvement of sulfhydryl ligands (from the reduction of a disulfide linkage) is argued against by the inability of borohydride and DTT, both suitable reducing agents for the reduction of disulfide linkages, to stimulate activation. Both dithionite and borohydride are capable of reducing Ni(II) to Ni(0) upon prolonged incubation, but borohydride is not capable of activating the apoenzyme (Table I), arguing against the involvement of Ni(0) in the activation process. The extreme instability of the Ni(I) ion, especially when uncomplexed and in aqueous solution (Cotton & Wilkinson, 1988), argues against its involvement in activation. The involvement of Ni(I) cannot, however, be unambiguously ruled out; ligation of Ni(II) to some but not all of the final site ligands may favorably change the potential of the Ni(II)/Ni(I) couple, leading to reduction to Ni(I) and completion of the nickel coordination sphere.

The mode of ligation of nickel to the apoenzyme is of interest in light of the observation that the oxidized enzyme is not a substrate for activation. To date, little structural information on the nature of the nickel center of CO dehydrogenase is available. EPR (Bonam & Ludden, 1987; Bonam et al., 1988) and UV/visible (Bonam & Ludden, 1987; Ensign et al., 1989a) spectroscopy has demonstrated that *R. rubrum* CO dehydrogenase contains Fe–S centers which appear to be identical in the apo- and holoenzymes. EPR temperature and power saturation studies on the dithionite-reduced enzymes indicate the presence of two Fe_4–S_4 centers (Bonam & Ludden, 1987; Bonam et al., 1988). The holoenzyme contains an additional paramagnetic center (g values of 2.04, 1.90, and 1.71) observed only in the dye-oxidized form of the enzyme, and this signal is completely lacking in dye-oxidized apo-CO dehydrogenase (Stephens et al., 1989). This novel EPR signal is completely restored to the apoenzyme upon activation by $NiCl_2$ and exhibits broadening upon isotopic substitution of ^{61}Ni or ^{57}Fe, demonstrating that nickel and iron are closely coupled in the enzyme, and possibly interact in a distinct iron–nickel center (Stephens et al., 1989).

Perhaps nickel forms a complex by ligating both with a peptide portion of the enzyme and additionally with one (or both) of the Fe_4–S_4 centers of the apoenzyme by sharing a sulfur atom (cysteine or inorganic sulfide). Alternatively, nickel may insert into a vacant site of a preformed, as yet uncharacterized Fe–S center to form a distinct, heterogeneous cluster containing both iron and nickel. EXAFS and magnetic circular dichroism studies of both apo- and holo-CO dehydrogenase are currently in progress and should shed light on the nature of the nickel center.

The first-order and initial rate kinetic analyses of apo-CO dehydrogenase activation reveal that activation is a pseudo-first-order process which exhibits saturation kinetics. The saturable nature of the activation implies a two-step mechanism, in which the enzyme reversibly binds nickel to form a loosely bound enzyme–nickel complex, with nickel then "seating" to form the active and stable holoenzyme (Scheme I).

The equilibrium between E, Ni, and E·Ni is rapidly established and represented by K_D:

$$K_D = k_2/k_1 = [E][Ni]/[E{\cdot}Ni] \quad (5)$$

The rate of conversion of the inactive (E·Ni) complex to the active (E·Ni*) complex is dictated by the value of k_{max} (0.157 min^{-1}):

$$d(E{\cdot}Ni^*)/dt = k_{max}(E{\cdot}Ni) \quad (6)$$

Step 2 in Scheme I may, for example, involve a conformational change at the active site of the enzyme (induced by the initial binding of nickel) which allows nickel to bind in the correct configuration to produce the holoenzyme. The conversion of E·Ni to E·Ni* is most likely an essentially irreversible process, based on the observations that the activity of the activated apoenzyme or the purified holoenzyme is stable to incubation with the inhibitory metal ions cobalt, zinc, and iron or the metal chelators EDTA and dimethylglyoxime (Ensign and Ludden, unpublished experiments). The interrelationship between k_{max}, K_D, and the pseudo-first-order rate constants (k_{obs}) obtained for a given concentration of nickel may be represented by

$$k_{obs} = \frac{k_{max}[Ni]}{K_D + [Ni]} \quad (7)$$

Surprisingly, the transition metals which are inhibitors of activation (cadmium, zinc, cobalt, and iron) apparently bind the purified enzyme from 2–300 times tighter than nickel (see Table II). This contrasts the results obtained in in vivo experiments; iron is not incorporated into the nickel site of CO dehydrogenase when cells are grown on nickel-deficient medium, and preliminary experiments indicate that very little cobalt associates with CO dehydrogenase when cells are grown on nickel-deficient medium supplemented with 50 μM $CoCl_2$ (Ensign and Ludden, unpublished experiments). These results suggest that *R. rubrum* contains highly specific nickel uptake and/or insertion processes which assure that nickel is incorporated into the apoenzyme in vivo.

Acknowledgments

We thank Dr. Vinod Shah for providing us with *A. vinelandii* flavodoxin, Dr. Duane Bonam for providing *C. pasteurianum* hydrogenase I, and Scott Murrell for providing *R. rubrum* ferredoxins I and II. We thank Professors W. W. Cleland and P. J. Stephens for useful discussions and W. W. Cleland and Vinod Shah for their careful readings of the manuscript.

Registry No. CODH, 64972-88-9; Ni, 7440-02-0; Cd, 7440-43-9; Zn, 7440-66-6; Co, 7440-48-4; Fe, 7439-89-6; sodium dithionite, 7775-14-6; reduced methylviologen, 15591-62-5.

References

Bonam, D., & Ludden, P. W. (1987) *J. Biol. Chem. 262*, 2980–2987.

Bonam, D., McKenna, M. C., Stephens, P. J., & Ludden, P. W. (1988) *Proc. Natl. Acad. Sci. U.S.A. 85*, 31–35.

Bonam, D., Lehman, L., Roberts, G. P., & Ludden, P. W. (1989) *J. Bacteriol. 171*, 3102–3107.

Clark, W. M. (1960) *Oxidation–Reduction Potentials of Organic Systems*, p 409, Williams & Wilkin, Baltimore.

Cleland, W. W. (1964) *Biochemistry 3*, 480–482.

Cleland, W. W. (1979) *Methods Enzymol. 63*, 103–138.

Cotton, F. A., & Wilkinson, G. (1988) *Advanced Inorganic Chemistry*, 5th ed., p 754, Wiley, New York.

Dutton, P. L. (1978) *Methods Enzymol. 54*, 411–435.

Ensign, S. A., Bonam, D., & Ludden, P. W. (1989a) *Biochemistry 28*, 4968–4973.

Ensign, S. A., Hyman, M. R., & Ludden, P. W. (1989b) *Biochemistry 28*, 4973–4979.

Hausinger, R. P. (1987) *Microbiol. Rev. 51*, 22–42.

Krzycki, J. A., & Zeikus, J. G., (1984) *J. Bacteriol. 158*, 231-237.
Mobley, H. L. T., & Hausinger, R. P. (1989) *Microbiol. Rev. 53*, 85-108.
Peterson, G. L. (1977) *Anal. Biochem. 83*, 346-356.
Prince, R. C., Linkletter, S. J. G., & Dutton, P. L. (1981) *Biochim. Biophys. Acta 635*, 132-148.
Saint-Martin, P., Lespinat, P. A., Fauque, G., Berlier, Y., LeGall, J., Moura, I., Teixeira, M., Xavier, A. V., & Moura, J. J. G. (1988) *Proc. Natl. Acad. Sci. U.S.A. 85*, 9378-9380.
Stephens, P. J., McKenna, M. C., Ensign, S. A., Bonam, D., & Ludden, P. W. (1989) *J. Biol. Chem. 264*, 16347-16350.
Terlesky, K. C., Nelson, M. J. K., & Ferry, J. G. (1986) *J. Bacteriol. 168*, 1053-1058.
Walsh, C. T., & Orme-Johnson, W. H. (1987) *Biochemistry 26*, 4901-4906.
Wood, H. G., Ragsdale, S. W., & Pezacka, E. (1986) *Biochem. Int. 12*, 421-440.

Purification to Homogeneity and Properties of Mannosidase II from Mung Bean Seedlings†

Gur P. Kaushal, T. Szumilo,‡ Irena Pastuszak, and Alan D. Elbein*
Department of Biochemistry, University of Texas Health Science Center, San Antonio, Texas 78284
Received August 9, 1989; Revised Manuscript Received October 25, 1989

ABSTRACT: Mannosidase II was purified from mung bean seedlings to apparent homogeneity by using a combination of techniques including DEAE-cellulose and hydroxyapatite chromatography, gel filtration, lectin affinity chromatography, and preparative gel electrophoresis. The release of radioactive mannose from GlcNAc[^{3}H]Man_5GlcNAc was linear with time and protein concentration with the purified protein, did not show any metal ion requirement, and had a pH optimum of 6.0. The purified enzyme showed a single band on SDS gels that migrated with the M_r 125K standard. The enzyme was very active on GlcNAcMan_5GlcNAc but had no activity toward Man_5GlcNAc, Man_9GlcNAc, Glc_3Man_9GlcNAc, or other high-mannose oligosaccharides. It did show slight activity toward Man_3GlcNAc. The first product of the reaction of enzyme with GlcNAcMan_5GlcNAc, i.e., GlcNAcMan_4GlcNAc, was isolated by gel filtration and subjected to digestion with endoglucosaminidase H to determine which mannose residue had been removed. This GlcNAcMan_4GlcNAc was about 60% susceptible to Endo H indicating that the mannosidase II preferred to remove the α1,6-linked mannose first, but 40% of the time removed the α1,3-linked mannose first. The final product of the reaction, GlcNAcMan_3GlcNAc, was characterized by gel filtration and various enzymatic digestions. Mannosidase II was very strongly inhibited by swainsonine and less strongly by 1,4-dideoxy-1,4-imino-D-mannitol. It was not inhibited by deoxymannojirimycin.

The biosynthesis of the oligosaccharide chains of the N-linked glycoproteins of plant cells, like those of animal cells, involves two series of reactions. The first series of reactions gives rise to the common intermediate that is the precursor for all of the N-linked oligosaccharides. In these reactions, the individual sugars, GlcNAc, mannose, and glucose, are added sequentially to the lipid carrier, dolichyl-P, to form the precursor lipid-linked oligosaccharide, $Glc_3Man_9(GlcNAc)_2$-PP-dolichol, which then serves as the donor of oligosaccharide to certain asparagine residues on the protein (Struck & Lennarz, 1980; Elbein, 1979; Staneloni & Leloir, 1982). Oligosaccharide transfer is a cotranslational event and occurs in the endoplasmic reticulum of the cell while the protein is still being synthesized on membrane-bound polysomes (Kiely et al., 1976; Lingappa et al., 1978; Rothman & Lodish, 1977).

Once the oligosaccharide has been transferred to protein, a series of reactions occur that result in modifications of the oligosaccharide chains to give rise to the various types of N-linked structures (Hunt et al., 1978; Hubbard & Ivatt, 1981). These reactions, which are referred to as processing reactions, are fairly well documented in animal cells, and many of the enzymes have been highly purified, but they are not nearly as well understood in plant cells (Elbein, 1988). The initial reactions of this processing pathway begin in the endoplasmic reticulum (ER), probably while the protein is still being synthesized. Two membrane-bound glucosidases, called glucosidase I and glucosidase II, remove the three glucoses to give a $Man_9(GlcNAc)_2$-protein. Glucosidase I removes the outermost α1,2-linked glucose (Grinna & Robbins, 1979; Hettkamp et al., 1984; Shailubhai et al., 1987) while glucosidase II removes the next two α1,3-linked glucoses (Michael & Kornfeld, 1980; Burns & Touster, 1982; Martiniuk et al., 1985; Brada & Dubach, 1984). The resulting $Man_9(GlcNAc)_2$ structure may remain as a high-mannose type, or it may be further modified in the ER and in the Golgi. There are several recently described enzymes found in animal cells that can act on these N-linked glycoproteins, but their exact role or function in the processing pathway is unclear at this time. For example, an α-mannosidase has been demonstrated in the ER that can remove a single or several of the α1,2-linked mannose residues to give $Man_{6-8}(GlcNAc)_2$-glycoproteins (Bischoff et al., 1986). There is also an endomannosidase in the Golgi of some animal cells that cleaves a glucosyl-α1,3-mannose from the $Glc_1Man_9(GlcNAc)_2$-protein to give a $Man_8(GlcNAc)_2$-protein (Lubas & Spiro, 1988). Once the protein enters the cis-Golgi as the $Man_{8-9}(GlcNAc)_2$-protein, it can be trimmed by

†This study was supported by grants from the National Institutes of Health (NIH DK 21800) and from the Robert A. Welch Foundation.
*To whom correspondence should be addressed.
‡Present address: Department of Biochemistry, Medical School, Lublin, Poland.

0006-2960/90/0429-2168$02.50/0